Coated nonmagnetic spheres with a negative index of refraction at infrared frequencies

Mark S. Wheeler,* J. Stewart Aitchison, and Mohammad Mojahedi
The Edward S. Rogers Sr. Department of Electrical and Computer Engineering,
University of Toronto, 10 King's College Road, Toronto, Ontario, Canada, M5S 3G4
(Received 4 October 2005; revised manuscript received 28 November 2005; published 6 January 2006)

A three-dimensional lattice of micron-scale coated spheres is shown to have an isotropic negative index of refraction at infrared frequencies. The materials used are entirely non-magnetic. The Mie scattering theory of the constituent spheres is used in the effective medium theory. The physical mechanisms and procedures are presented in the design of a negative effective permeability with solid polaritonic spheres, as well as a negative effective permittivity with solid Drude spheres. It is then shown that a collection of polaritonic spheres coated with a thin layer of Drude material can exhibit a negative index of refraction at infrared frequencies. Comparison with numerical photonic band structure calculations verifies the theory.

DOI: 10.1103/PhysRevB.73.045105 PACS number(s): 78.20.Ci, 41.20.Jb, 42.30.−d, 42.70.Qs

I. INTRODUCTION

There has been much progress in the development of negative-index metamaterials in the past few years. This progress, however, has been much more rapid for metamaterials which operate at microwave frequencies than for those at infrared and optical frequencies. The first negative-index metamaterials[1,2] combined arrays of thin metal wires, which provide a negative permittivity,[3] and split-ring resonators, which provide a negative permeability.[4] Although split-ring resonators have been scaled down to micron-scale features which operate at far-infrared frequencies,[5] they become very difficult to fabricate at these dimensions. Additionally, their inherent anisotropy requires that an isotropic metamaterial have a three-dimensionally orthogonal arrangement. Loaded transmission line media[6,7] have proven quite useful in making compact microwave devices, but their reliance on lumped or distributed loading elements makes them unsuitable for optical frequencies. Photonic crystals can have a negative effective index, although the mechanism responsible for the effect is different, and as such they are more prone to practical problems.[8,9]

We are interested in developing negative-index metamaterials at infrared and optical frequencies. To this end, we have previously reported that a three-dimensional array of dielectric spheres can be made to exhibit an isotropic negative permeability.[10,11] The background theory of the effective permittivity and permeability of dielectric and magnetic spheres was first reported by Lewin.[12] Other reports have also found a negative permeability or negative index by using magnetodielectric[13] or ferroelectric[14] spheres. In all of these cases, the magnetic response is excited by leaky cavity resonances in the spheres. These localized resonances can be lowered into the long-wavelength limit by using nonmagnetic spheres with a large permittivity. The localized nature of the resonances results in an isotropic negative permeability which does not depend on the exact lattice structure or Bragg scattering. These concepts were also used to predict a negative permeability in two-dimensional dielectric rods.[15,16] Most recently, a negative-index composite was reported[17] which used two interpenetrating lattices of spheres: one lattice used a polaritonic material to provide a negative permeability, and the other lattice used a Drude material to provide a negative permittivity.

Here we report on the design of a negative-index metamaterial made of a single lattice of nonmagnetic coated spheres. We extend the effective medium theory of Ref. 11 to accommodate the coated spheres and describe a design procedure. The spheres have a core of $LiTaO_3$, which is a polaritonic crystal. The core is coated by a thin layer of a Drude model semiconductor. The dimensions of the constituents are a few microns, which results in a negative index at infrared frequencies. Section II presents the effective medium theory and Mie scattering of dielectric spheres. Section III presents the methods of designing both a negative permeability and negative permittivity with solid spheres. In Sec. IV we show how coated spheres, which have modified Mie scattering coefficients, can have a negative index of refraction. We then verify our theory by comparing our results with photonic band calculations. Finally, the results are summarized in Sec. V.

II. EFFECTIVE MEDIUM THEORY

We now summarize the theory which relates the scattering from a small obstacle to the bulk permittivity and permeability of a collection of such obstacles.[11] We initially consider this obstacle to be a dielectric sphere. Section IV will discuss the modifications necessary for coated spheres. The following derivation concentrates on the magnetic fields; the dual relations are valid for the electric fields.

An incident plane wave, represented by the magnetic field $\mathbf{H}_{\text{inc}}=H_0 \exp(ik_0 z)\hat{\mathbf{y}}$ and $k_0=\omega/c$, is incident on a single isolated sphere of radius r_0 and relative permittivity $\epsilon_r=n^2$. The scattered magnetic field can be decomposed into multipole terms; the proportionality constant of the 2^m-pole term is[18]

$$b_m = \frac{\psi_m(nx)\psi_m'(x) - n\psi_m(x)\psi_m'(nx)}{\psi_m(nx)\xi_m'(x) - n\xi_m(x)\psi_m'(nx)}, \tag{1}$$

and the 2^m-pole coefficients of the scattered electric field are

 ©2006 The American Physical Society

$$a_m = \frac{n\psi_m(nx)\psi_m'(x) - \psi_m(x)\psi_m'(nx)}{n\psi_m(nx)\xi_m'(x) - \xi_m(x)\psi_m'(nx)}. \tag{2}$$

Here $x=k_0r_0$, and $\psi_m(z)=zj_m(z)$ and $\xi_m(z)=zh_m^{(1)}(z)$ relate the Riccati-Bessel functions to the spherical Bessel functions.[19] The primes indicate differentiation with respect to the argument. The scattered magnetic dipole field is proportional to b_1 and is given by[18]

$$\begin{aligned}\mathbf{H}_{\text{sca}} &= -\frac{3}{2}H_0b_1\left\{2\hat{\mathbf{r}}\sin\theta\sin\phi\frac{h_1^{(1)}(k_0r)}{k_0r} + (\hat{\boldsymbol{\theta}}\cos\theta\sin\phi + \hat{\phi}\cos\phi)\frac{[k_0rh_1^{(1)}(k_0r)]'}{k_0r}\right\}\\ &= \frac{3}{2}\frac{iH_0b_1}{k_0^3}\frac{e^{ik_0r}}{r}\left\{k_0^2(\hat{\mathbf{r}}\times\hat{\mathbf{y}})\times\hat{\mathbf{r}} + [3(\hat{\mathbf{y}}\cdot\hat{\mathbf{r}})\hat{\mathbf{r}} - \hat{\mathbf{y}}]\left(\frac{1}{r^2} - \frac{ik_0}{r}\right)\right\}.\end{aligned} \tag{3}$$

Note that all of the near-field terms have been retained. This expression may be compared with the standard expression of magnetic dipole radiation,[20]

$$\begin{aligned}\mathbf{H}_{\text{dipole}} = \frac{1}{4\pi}\frac{e^{ik_0r}}{r}&\left\{k_0^2(\hat{\mathbf{r}}\times\hat{\mathbf{m}})\times\hat{\mathbf{r}} + [3(\hat{\mathbf{m}}\cdot\hat{\mathbf{r}})\hat{\mathbf{r}} - \hat{\mathbf{m}}]\right.\\ &\left.\times\left(\frac{1}{r^2} - \frac{ik_0}{r}\right)\right\}.\end{aligned} \tag{4}$$

Therefore, we can conclude that the sphere is completely equivalent to a magnetic dipole with an effective moment $\mathbf{m}$ and effective polarizability α_m, where $\mathbf{m}=\alpha_m\mathbf{H}_{\text{inc}}(0) = \alpha_mH_0\hat{\mathbf{y}}$. The effective polarizability is then[21]

$$\alpha_m = 6\pi ib_1/k_0^3. \tag{5}$$

The response of a bulk material is described by the effective permeability μ_r^{eff}. The Clausius-Mossotti equation,[20] also known as the Lorentz-Lorenz formula,[22] relates the long-wavelength limit bulk effective permeability to the effective polarizability of the single sphere,

$$\alpha_m = \frac{3}{N}\left(\frac{\mu_r^{\text{eff}} - 1}{\mu_r^{\text{eff}} + 2}\right), \tag{6}$$

where N is the volume density of the spheres. The filling fraction f of the composite is $f=4\pi Nr_0^3/3$. Only modest filling fractions are considered here; large values require corrections due to higher-order multipole terms and structure-dependent lattice sums. Finally, substitution of Eq. (5) into Eq. (6) yields the effective permeability in terms of the first-order multipole term b_1,

$$\mu_r^{\text{eff}} = \frac{k_0^3 + 4\pi iNb_1}{k_0^3 - 2\pi iNb_1}. \tag{7}$$

Similarly, the effective permittivity ϵ_r^{eff} can be related to the scattered electric dipole term a_1,

$$\epsilon_r^{\text{eff}} = \frac{k_0^3 + 4\pi iNa_1}{k_0^3 - 2\pi iNa_1}. \tag{8}$$

Expressions (7) and (8) completely determine the response of the bulk composite. They depend on the frequency of the wave as well as the radius, density, and composition of the spheres.

III. COMPOSITE OF SOLID SPHERES

A collection of solid non-magnetic spheres can be designed to have almost arbitrary values of μ_r^{eff} and ϵ_r^{eff}. In this work we are particularly interested in designing negative-index materials, which requires both a negative permeability and a negative permittivity. Here we outline the design procedure for a separate negative permeability and negative permittivity; this will prove useful in the design of a negative index in Sec. IV.

A. Negative permeability

We reported the design of a negative permeability using dielectric spheres in Ref. 11. In this section the results of that report are summarized, along with additional design limits and procedures.

The magnetic response of a nonmagnetic composite requires appreciable values of the b_1 coefficient. Since the values of b_1 are usually small, it is important to investigate its resonant behavior. From Eq. (1), resonances are induced if

$$\frac{\xi_1'(x)}{\xi_1(x)} = n\frac{\psi_1'(nx)}{\psi_1(nx)}. \tag{9}$$

The pseudoperiodic nature of these functions implies that there are an infinite number of resonances. However, these resonances often occur at frequencies beyond the long-wavelength limit. Then the Clausius-Mossotti equation does not apply; those resonances do not contribute to μ_r^{eff}.

The resonant frequencies of b_1 that are within the long-wavelength limit can be estimated when x is small, although the value of nx is unrestricted. Then Eq. (9) reduces to

$$j_0(nx) = \frac{\sin(nx)}{nx} = 0, \tag{10}$$

which has the roots $nx = \pi q$ for $q = 1, 2, 3\ldots$. The fundamental magnetic resonant frequency ω_m^{res}, when $q = 1$, is

$$\omega_m^{\text{res}} = \frac{\pi c}{r_0\sqrt{\epsilon_r}}. \tag{11}$$

This can also be expressed as a ratio between the free-space wavelength and the diameter of the sphere,

$$\lambda_0^{\text{res}}/2r_0 = \sqrt{\epsilon_r}. \tag{12}$$

Assuming a definition of the long-wavelength limit of $\lambda_0^{\text{res}}/2r_0 > 10$, the permittivity of the spheres must satisfy $\epsilon_r > 100$ so that the magnetic resonance is within the long-wavelength limit. This result is not surprising when the sphere is viewed as a dielectric cavity; the frequency of the bulk resonance must be depressed into the long-wavelength limit of the ambient medium.

Ferroelectric or polaritonic materials can provide the required large dielectric constants. Whereas ferroelectrics may be more useful for resonances in the microwave range, the lattice resonance in polaritonic crystals (*reststrahlen* region) can be exploited to tailor the permeability resonance at infrared and optical frequencies. The relative permittivity of polaritonic materials follows the relation

$$\epsilon_r(\omega) = \epsilon(\infty)\left(1 + \frac{\omega_L^2 - \omega_T^2}{\omega_T^2 - \omega^2 - i\omega\gamma}\right), \tag{13}$$

where $\epsilon(\infty)$ is the high-frequency limit of the permittivity, ω_T is the transverse optical phonon frequency, ω_L is the longitudinal optical phonon frequency, and γ is the damping coefficient.[23] These parameters are related by the Lyddane-Sachs-Teller relation $\omega_L^2/\omega_T^2 = \epsilon(0)/\epsilon(\infty)$, where $\epsilon(0)$ is the static permittivity. The spheres in the following are assumed to be made of $LiTaO_3$, using the following parameters:[24] $\epsilon(0) = 41.4$, $\epsilon(\infty) = 13.4$, $\omega_T/2\pi = 4.25$ THz, $\omega_L/2\pi = 7.46$ THz, and $\gamma/2\pi = 0.15$ THz.

As an example,[11] consider a collection of $LiTaO_3$ spheres with filling fraction 0.268 and $r_0 = 4$ μm. Using Eq. (13) with $\gamma = 0$ in Eq. (11) leads to an estimate of the magnetic resonance frequency of $\omega_m^{\text{res}}/2\pi = 3.58$ THz, where the relative permittivity of $LiTaO_3$ is $\epsilon_r(\omega_m^{\text{res}}) = 109.8 + i1.57$. A full calculation of Eq. (7) reveals a resonance in μ_r^{eff} centered at 3.53 THz, which is very close to the previous prediction. A negative permeability is found above the resonance, which has a minimum real value of $\mu_r^{\text{eff}} = -0.25$ at 3.58 THz. These results, as well as a figure of μ_r^{eff}, were previously reported in Ref. 11. The details presented here are sufficient to assist in the design of a negative index metamaterial and will be needed in Sec. IV.

B. Negative permittivity

The method described in Sec. III A can also be used to find the resonances of the electric response a_1. The first electric resonance, however, is at a higher frequency than the fundamental magnetic resonance. This means that a sphere with an even larger dielectric constant than that found in Sec. III A would be required to drive such a bulk resonance. Fortunately, there is another mechanism by which an electric-dipole resonance can be induced. This can be seen from a series expansion of (2), for $m = 1$,[18]

$$a_1 = -i\frac{2}{3}\left(\frac{\epsilon_r - 1}{\epsilon_r + 2}\right)x^3 + \mathcal{O}(x^5). \tag{14}$$

An isolated sphere has an electric dipole resonance when its material permittivity $\epsilon_r = -2$. Note that since this value is negative, the fields are evanescent within the sphere, making this a surface resonance. This is in contrast to the magnetic resonance, which is a bulk cavity resonance.

How is ϵ_r^{eff} affected by the resonance in a_1? Using Eq. (14) in Eq. (8) and setting the resulting denominator to zero, the condition

$$\epsilon_r^{\text{res}} = \frac{f + 2}{f - 1} \tag{15}$$

approximates the material permittivity of the spheres that is required to drive a resonance in ϵ_r^{eff}. The required material permittivity is always negative and becomes more negative with increasing filling fraction.

Metals and semiconductors, which follow the Drude model dispersion, can provide the required negative material permittivity. The Drude model is given by

$$\epsilon_r(\omega) = 1 - \frac{\omega_p^2}{\omega^2 + i\omega\gamma}, \tag{16}$$

where ω_p is the plasma frequency and γ is the damping term. The resonance condition (15) indicates that it is the small negative values of permittivity that are of interest, which occur just below ω_p in Eq. (16). Metals typically have plasma frequencies in the ultraviolet and are not useful here. Instead, semiconductor materials can be tailored to provide the required plasma frequencies in the infrared. Note that one could also choose polaritonic materials.

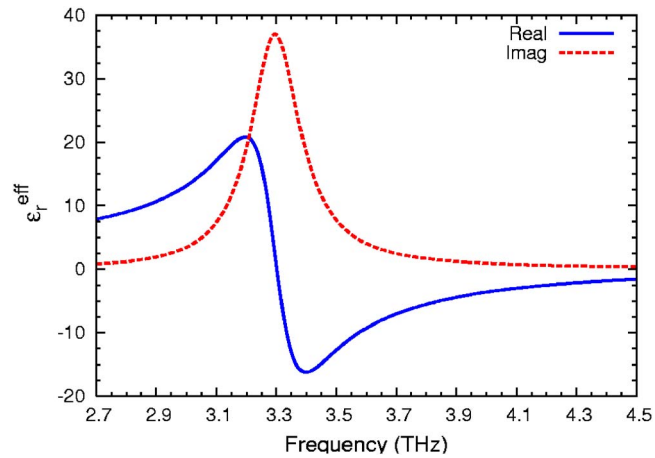

FIG. 1. (Color online) The effective permittivity of a collection of spheres with filling fraction $f = 0.435$ and radius $r_0 = 4.7$ μm. The spheres are made of a Drude material with $\omega_p/2\pi = 8.13$ THz and $\gamma = \omega_p/100$.

The required plasma frequency of the material can be approximated by equating Eqs. (15) and (16) and letting $\gamma \to 0$, which yields

$$\omega_p = \omega_e^{\text{res}} \sqrt{\frac{3}{1-f}}, \tag{17}$$

where ω_e^{res} is the desired resonance frequency of ϵ_r^{eff}. As an example, if $f=0.435$ and we specify a resonant frequency of $\omega_e^{\text{res}}/2\pi=3.53$ THz (the same resonant frequency as Sec. III A), then the required plasma frequency of the material is $\omega_p/2\pi=8.13$ THz. For simplicity, these approximations have not included losses; we may now use[16] $\gamma=\omega_p/100$ in Eq. (16) and calculate the effective media parameters using Eqs. (7) and (8). These Drude model values could be achieved with doped semiconductors. The calculated ϵ_r^{eff} is shown in Fig. 1. The values for μ_r^{eff} for this system do not vary significantly from unity and are not shown.

IV. COMPOSITE OF COATED SPHERES

A. Negative index of refraction

A negative index of refraction requires both a negative permeability and permittivity at the same frequency. Section III A described how to design a negative permeability, and Sec. III B described how to design a negative permittivity. Unfortunately, both cannot be made negative in the same frequency range. Nevertheless, the same concepts can be applied to more complex structures. We solve this problem by now considering coated spheres. In particular, we choose to tune the core to provide $\mu_r^{\text{eff}}<0$ and the coating to provide $\epsilon_r^{\text{eff}}<0$. Figure 2 shows a schematic of the coated sphere, which has a core in the region $0<r<r_1$ with index $n_1=\epsilon_1^2$ and a coating in the region $r_1<r<r_2$ with index $n_2=\epsilon_2^2$. The scattering coefficients (1) and (2) no longer apply, and must be modified. The appropriate equations, whose derivation may be found in Ref. 18, are

$$b_m = \frac{n_2\psi_m(y)[\psi_m'(n_2y)-B_m\chi_m'(n_2y)]-\psi_m'(y)[\psi_m(n_2y)-B_m\chi_m(n_2y)]}{n_2\xi_m(y)[\psi_m'(n_2y)-B_m\chi_m'(n_2y)]-\xi_m'(y)[\psi_m(n_2y)-B_m\chi_m(n_2y)]}, \tag{18}$$

$$B_m = \frac{n_2\psi_m(n_1x)\psi_m'(n_2x)-n_1\psi_m(n_2x)\psi_m'(n_1x)}{n_2\chi_m'(n_2x)\psi_m(n_1x)-n_1\psi_m'(n_1x)\chi_m(n_2x)}, \tag{19}$$

$$a_m = \frac{\psi_m(y)[\psi_m'(n_2y)-A_m\chi_m'(n_2y)]-n_2\psi_m'(y)[\psi_m(n_2y)-A_m\chi_m(n_2y)]}{\xi_m(y)[\psi_m'(n_2y)-A_m\chi_m'(n_2y)]-n_2\xi_m'(y)[\psi_m(n_2y)-A_m\chi_m(n_2y)]}, \tag{20}$$

$$A_m = \frac{n_2\psi_m(n_2x)\psi_m'(n_1x)-n_1\psi_m'(n_2x)\psi_m(n_1x)}{n_2\chi_m(n_2x)\psi_m'(n_1x)-n_1\chi_m'(n_2x)\psi_m(n_1x)}, \tag{21}$$

where $x=k_0r_1$, $y=k_0r_2$, $\chi_m(z)=-zy_m(z)$, and $y_m(z)$ is the spherical Bessel function of the second kind.[19] To find the effective media values for coated spheres, we simply substitute these equations in Eqs. (7) and (8).

We will consider the core to be the same as the design in Sec. III A, which provides $\mu_r^{\text{eff}}<0$. A coating provides further conditions which allow a separately designable permittivity resonance. The magnetic resonance of the core is hardly affected, as long as the permittivity of the coating remains small in comparison to the large permittivity of the core. Just as in Sec. III B, the coating will be designed to have an electric-dipole resonance on its outer surface. However, the evanescent field within the coating can tunnel into the core, which will alter the resonance condition (15). Let us investigate this situation in the same manner as Sec. III B.

Given that the permittivity of the core is much larger than that of the coating—i.e., $|\epsilon_2/\epsilon_1|\to 0$—Eq. (20) can be approximated for $m=1$ according to

$$a_1 = -i\frac{2}{3}\left[\frac{(2\tau+1)\epsilon_2-(1-\tau)}{(2\tau+1)\epsilon_2+2(1-\tau)}\right]r_2^3k_0^3+\mathcal{O}(k_0^5), \tag{22}$$

where $\tau=(r_1/r_2)^3$. Therefore, the electric-dipole resonance condition for a single coated sphere with high-permittivity core requires that the coating material have a permittivity of

$$\epsilon_2^{\text{res}} = -2\left(\frac{1-\tau}{1+2\tau}\right). \tag{23}$$

Note that the resonance condition $\epsilon_2^{\text{res}}=-2$ for a solid sphere [see Eq. (14)] is recovered when $\tau\to 0$.

When a collection of coated spheres are brought together to make a composite with filling fraction $f=4\pi Nr_2^3/3$, the effective permittivity (23) will be modified. To find this new requirement on the coating permittivity ϵ_2^{res}, we substitute Eq. (22) in Eq. (8) and set the denominator to zero. The resonance in ϵ_r^{eff} occurs when the permittivity of the coating is

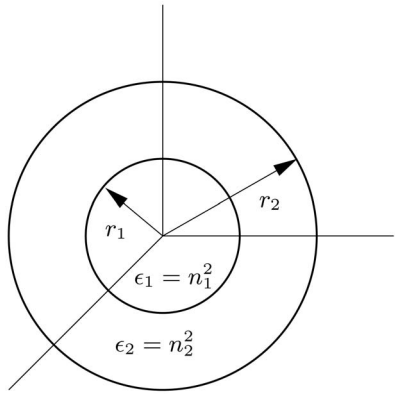

FIG. 2. A schematic of the coated sphere.

$$\epsilon_2^{\text{res}} = \left(\frac{f+2}{f-1}\right)\left(\frac{1-\tau}{1+2\tau}\right). \tag{24}$$

Equating Eq. (24) with Eq. (16) and letting $\gamma \to 0$ gives an estimate of the required plasma frequency of the coating material:

$$\omega_p = \omega_e^{\text{res}} \sqrt{\frac{3(1-\tau f)}{(1-f)(1+2\tau)}}. \tag{25}$$

Note that Eqs. (24) and (25), which are valid for coated spheres, reduce to the solid sphere results (15) and (17), when $\tau \to 0$. We have chosen the system parameters to be $r_1 = 4$ μm, $r_2 = 4.7$ μm, and $f = 0.435$. The effective permeability should have a resonance at the same frequency as the solid spheres designed in Sec. III A—namely, $\omega_m^{\text{res}}/2\pi = 3.58$ THz. The resonant frequency of the permittivity, however, does not need to be at this frequency. Indeed, by choosing a slightly lower ω_e^{res}, the permittivity resonance, which is much stronger and wider, will then have a lower loss at the magnetic resonance frequency. We therefore have chosen $\omega_e^{\text{res}}/2\pi = 3.2$ THz. Using this in Eq. (25) gives $\omega_p/2\pi = 4.22$ THz.

The full calculations of the effective permeability, permittivity, and index are shown in Fig. 3, complete with the inclusion of a Drude loss term of $\gamma = \omega_p/100$. The effective index was calculated with $n_{\text{eff}} = n'_{\text{eff}} + i n''_{\text{eff}} = \sqrt{\mu_r^{\text{eff}} \epsilon_r^{\text{eff}}}$ and ensuring that $n''_{\text{eff}} \geq 0$. The negative index region has a 9.8% bandwidth, centered at 3.61 THz. Also note that the value $n'_{\text{eff}} = -1$ is shown, which is an important criterion for subwavelength focusing.[25] The imaginary part of the index is proportional to attenuation and has moderate values in this range. The presence of loss is an inevitable consequence of the underlying resonances, but the losses are smaller at frequencies away from the center of the lines. The staggered overlap of the absorption lines of the permeability and permittivity is manifested in the effective index and is easily distinguished in Fig. 3(c). The need to lower the frequency of the stronger permittivity resonance in order to minimize n''_{eff} in the negative-index region should now be obvious. Finally, note that the imaginary parts of the calculated permittivity and permeability shown in Fig. 3 are always positive; the structure is definitely passive.[11]

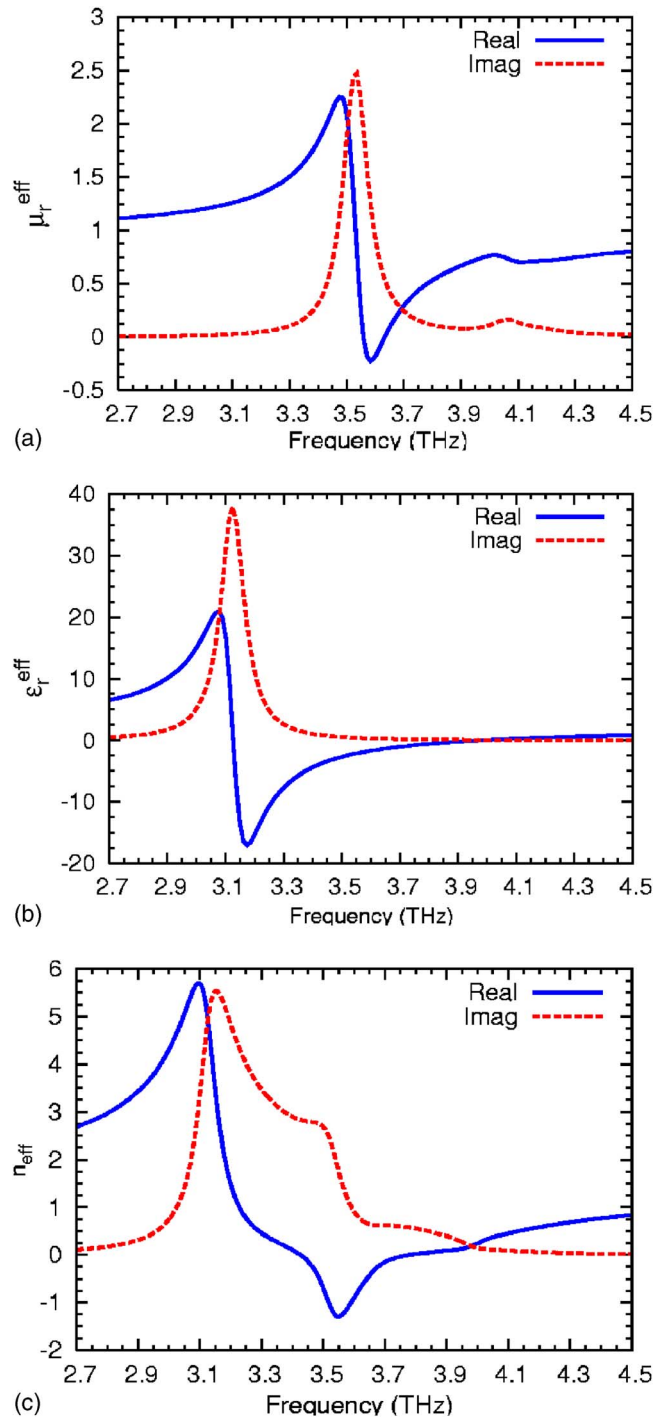

FIG. 3. (Color online) The effective (a) permeability, (b) permittivity, and (c) index of a collection coated spheres. The cores are made of $LiTaO_3$ of radius $r_1 = 4$ μm, and the coatings are a Drude material with $r_2 = 4.7$ μm, $\omega_p/2\pi = 4.22$ THz, and $\gamma = \omega_p/100$. The filling fraction is $f = 0.435$.

B. Band calculation and verification

Our results can be verified by comparing the effective dispersion relation, calculated with $k = \omega n_{\text{eff}}(\omega)/c$, and full numerical photonic band calculations. To this end, we have modified the code MULTEM2, which is available from Ref. 26. This code uses a scattering matrix technique which takes into

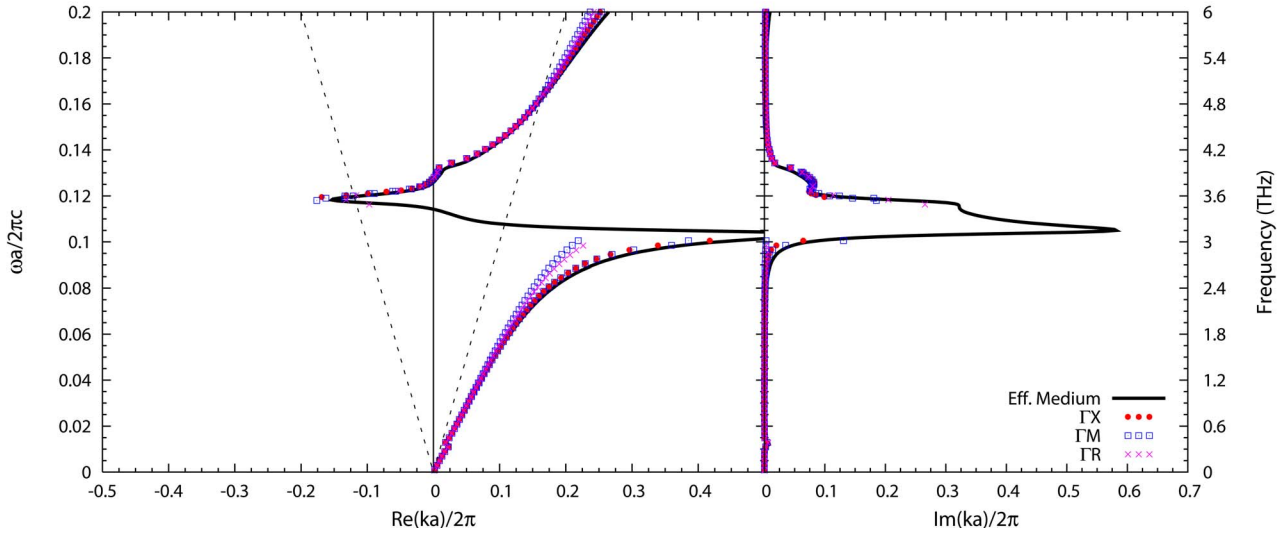

FIG. 4. (Color online) The real (band structure) and imaginary (attenuation) parts of the dispersion relation of a simple cubic lattice of coated spheres with lattice constant $a=10$ μm. The solid lines are calculated from the effective media theory, and the various point styles indicate the results of photonic band calculations for wave vectors along the canonical reciprocal lattice directions. The structure is the same as that described in Fig. 3.

account the multiple scattering between spheres arranged in a crystal lattice. Our modifications to the code include the polaritonic and Drude dispersion of the materials, as well as the a_m and b_m coefficients of the coated spheres. We consider the coated spheres to be arranged in a simple cubic lattice, so that the density $N=1/a^3$ makes the lattice constant of $a=10$ μm equivalent to the filling fraction $f=0.435$. Figure 4 compares the dispersion of the effective media theory with the band structure calculations with the wave vector fixed along the ΓX, ΓM, and ΓR directions. The real part of the band structure is symmetric about the origin; for clarity, the second branch is not shown. The curves verify our design and our effective media theory, as well as the isotropy of the composite. The modes with large attenuation in the anomalous dispersion region are not shown; they are of little importance here and are difficult to find with the code. The modes along ΓX and ΓR are doubly degenerate, whereas those along ΓM are nondegenerate, although they mostly overlap. The largest deviations between the curves occur just below the first resonance, where higher-order corrections might improve the theory.

The phase velocity $v_p=\omega/k$ and group velocity $v_g=\partial\omega/\partial k$ can be calculated from the real part of the band structure in Fig. 4. The anomalous dispersion region is between $0.103<\omega a/2\pi c<0.118$, where the group velocity is negative and there is large attenuation.[27] The negative-index region is found where the curves cross the origin between $0.114<\omega a/2\pi c<0.126$ (note that $k=\omega n_{\text{eff}}/c<0$). Backward waves, defined by $v_p<0$ and $v_g>0$, are found at the high-frequency end of this range, where $0.118<\omega a/2\pi c<0.126$. The negative index of refraction overlaps both the anomalous disperion region and the backward wave region.[27] However, it is this backward wave region, in the passband of the medium, that is commonly thought of as a negative index of refraction region.

V. SUMMARY

We have shown that a medium consisting of coated spheres can have a negative index of refraction. We have used Mie scattering theory in an effective medium approach which accurately predicts the effective dispersion of the composite. Design procedures have been elucidated for all cases of negative permeability, negative permittivity, and negative index. The structures presented are simple alternative designs of metamaterials at infrared frequencies.

Future work will investigate the fabrication of the presented structure. We note that, for example, nanocrystals of coated or onion-structure spheres with diameters as small as 20 nm have been fabricated with other materials,[28] so it is anticipated that the comparatively larger coated spheres presented here could be made as well. We emphasize that because of the long-wavelength limit approximation, an exact crystal lattice or high-degree of periodicity should not be necessary for the present structure; it is the filling fraction f, or equivalently the sphere density N, which has more importance, as shown in Eqs. (7) and (8).

ACKNOWLEDGMENTS

This work was supported by the Natural Sciences and Engineering Research Council of Canada under Grant No. 249531-02 and in part by Photonic Research Ontario, Funded Research No. 72022792.

*Electronic address: mark.wheeler@utoronto.ca

[1] D. R. Smith, W. J. Padilla, D. C. Vier, S. C. Nemat-Nasser, and S. Schultz, Phys. Rev. Lett. **84**, 4184 (2000).
[2] R. A. Shelby, D. R. Smith, and S. Schultz, Science **292**, 77 (2001).
[3] J. B. Pendry, A. J. Holden, W. J. Stewart, and I. Youngs, Phys. Rev. Lett. **76**, 4773 (1996).
[4] J. B. Pendry, A. J. Holden, D. J. Robbins, and W. J. Stewart, IEEE Trans. Microwave Theory Tech. **47**, 2075 (1999).
[5] T. J. Yen, W. J. Padilla, N. Fang, D. C. Vier, D. R. Smith, J. B. Pendry, D. N. Basov, and X. Zhang, Science **303**, 1494 (2004).
[6] O. F. Siddiqui, M. Mojahedi, and G. V. Eleftheriades, IEEE Trans. Antennas Propag. **51**, 2619 (2003).
[7] G. V. Eleftheriades, A. K. Iyer, and P. C. Kremer, IEEE Trans. Microwave Theory Tech. **50**, 2702 (2002).
[8] M. Notomi, Phys. Rev. B **62**, 10696 (2000).
[9] M. S. Wheeler, J. S. Aitchison, and M. Mojahedi, Phys. Rev. B **71**, 155106 (2005).
[10] M. S. Wheeler, J. S. Aitchison, and M. Mojahedi, in *Proceedings of IASTED Conference on Antennas, Radar, and Wave Propagation, Banff, Canada, 2005* (Acta Press, Calgary, AB, Canada), 475-143.
[11] M. S. Wheeler, J. S. Aitchison, and M. Mojahedi, Phys. Rev. B **72**, 193103 (2005).
[12] L. Lewin, Proc. Inst. Electr. Eng. **94**, 65 (1947).
[13] C. L. Holloway, E. F. Kuester, J. Baker-Jarvis, and P. Kabos, IEEE Trans. Antennas Propag. **51**, 2596 (2003).
[14] O. G. Vendik and M. S. Gashinova, in *Proceedings of the 34th European Microwave Conference, Amsterdam, 2004* (IEEE Press, Piscataway, NJ), Vol. 3, pp. 1209–1212.
[15] S. O'Brien and J. B. Pendry, J. Phys.: Condens. Matter **14**, 4035 (2002).
[16] K. C. Huang, M. L. Povinelli, and J. D. Joannopoulos, Appl. Phys. Lett. **85**, 543 (2004).
[17] V. Yannopapas and A. Moroz, J. Phys.: Condens. Matter **17**, 3717 (2005).
[18] C. F. Bohren and D. R. Huffman, *Absorption and Scattering of Light by Small Particles* (Wiley-Interscience, New York, 1983).
[19] *Handbook of Mathematical Functions with Formulas, Graphs, and Mathematical Tables*, edited by M. Abramowitz and I. A. Stegun (Dover, New York, 1972).
[20] J. D. Jackson, *Classical Electrodynamics*, 3rd ed. (Wiley, New York, 1999).
[21] W. T. Doyle, Phys. Rev. B **39**, 9852 (1989).
[22] M. Born and E. Wolf, *Principles of Optics: Electromagnetic Theory of Propagation, Interference and Diffraction of Light*, 7th ed. (Cambridge University Press, Cambridge, UK, 2002).
[23] C. Kittel, *Introduction to Solid State Physics*, 7th ed. (Wiley, New York, 1996).
[24] M. Schall, H. Helm, and S. R. Keiding, Int. J. Infrared Millim. Waves **20**, 595 (1999).
[25] J. B. Pendry, Phys. Rev. Lett. **85**, 3966 (2000).
[26] N. Stefanou, V. Yannopapas, and A. Modinos, Comput. Phys. Commun. **132**, 189 (2000).
[27] J. F. Woodley and M. Mojahedi, Phys. Rev. E **70**, 046603 (2004).
[28] L. M. Liz-Marzán and P. Mulvaney, J. Phys. Chem. B **107**, 7312 (2003).